Fig05.jpg.

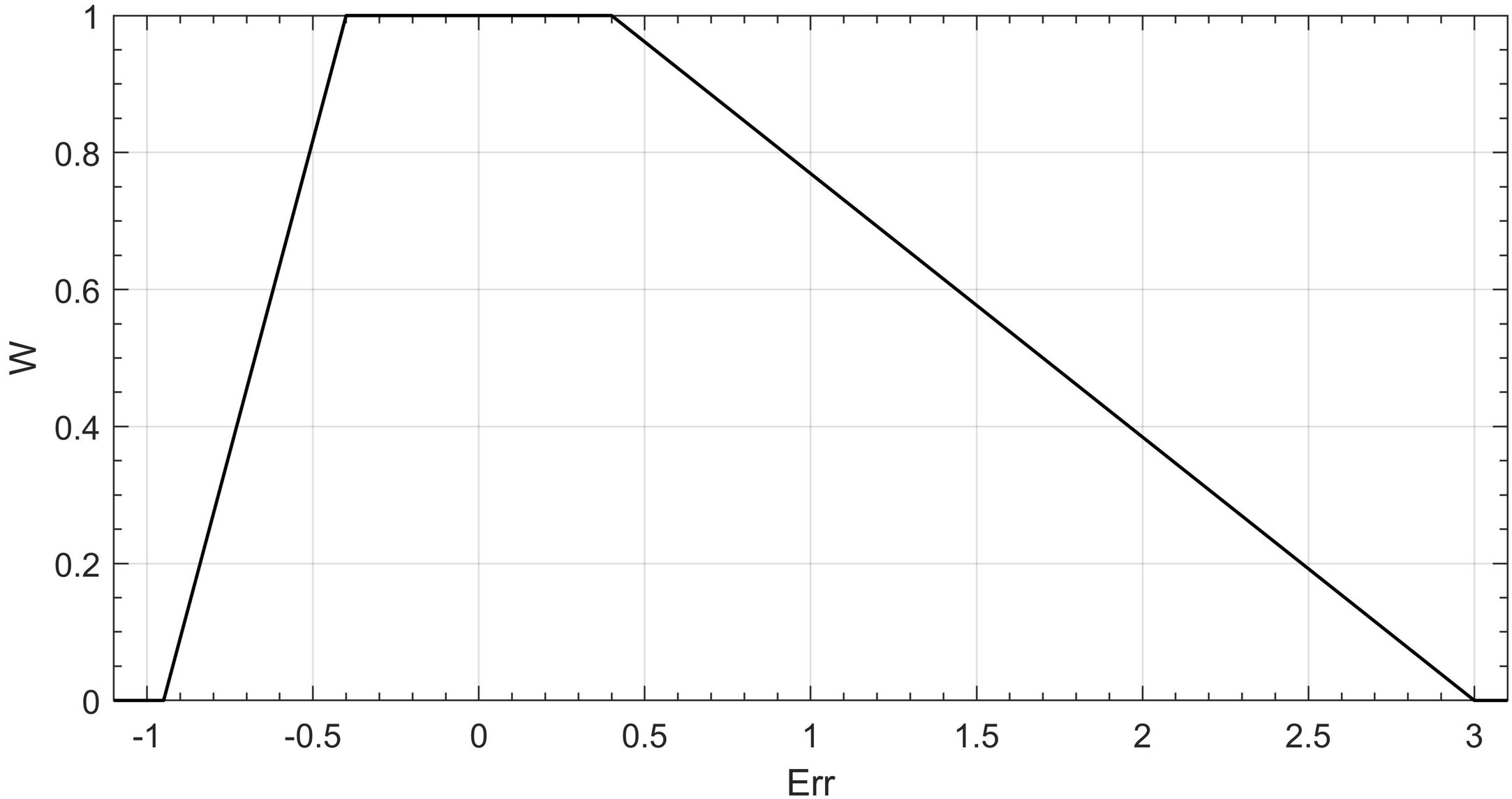
1
0.8
0.6
0.4
0.2
0
W
-1
-0.5
0
0.5
1
1.5
2
2.5
3
Err

Fig11.jpg.

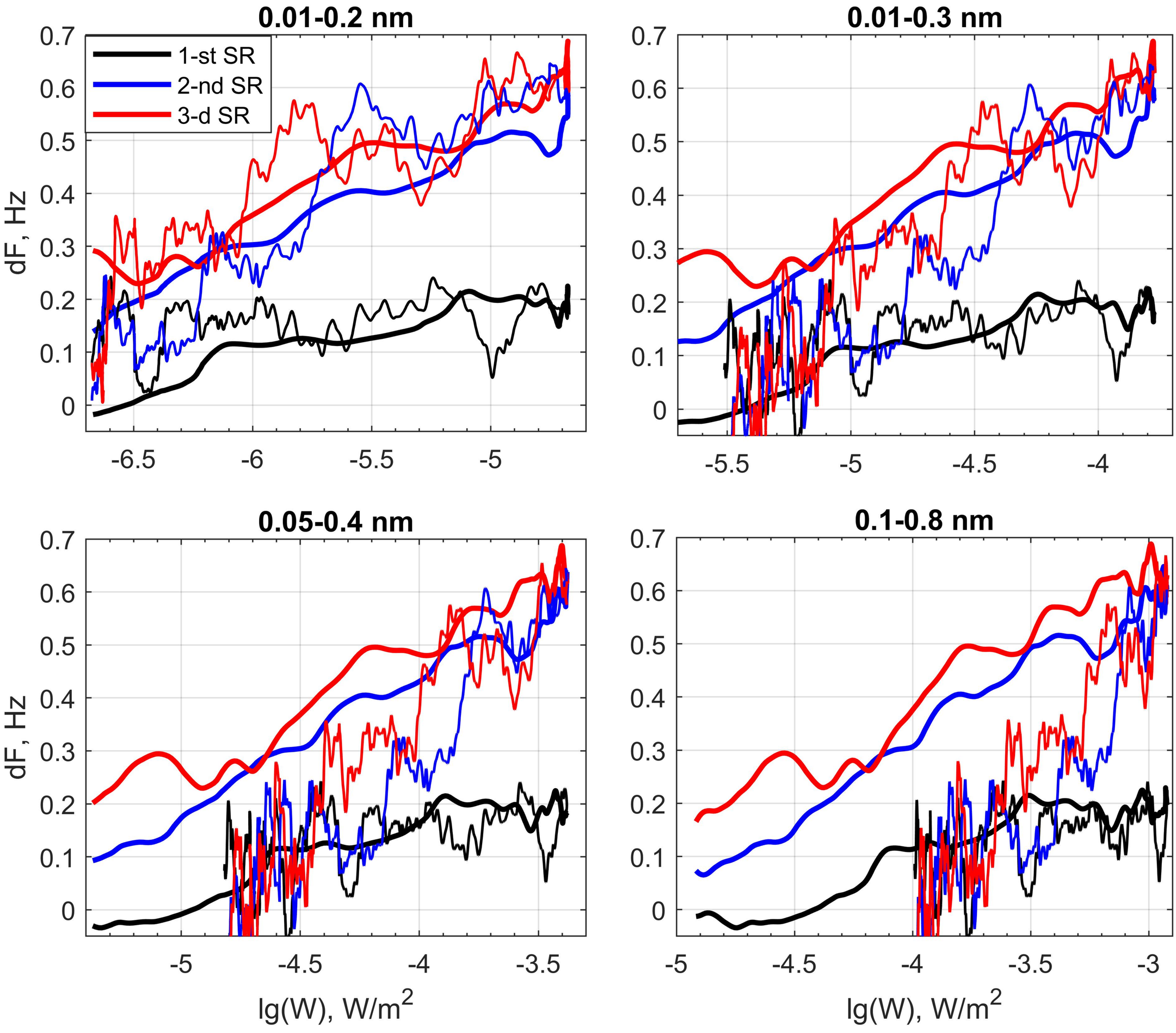
0.01-0.2 nm
0.01-0.3 nm
0.05-0.4 nm
0.1-0.8 nm
1-st SR
2-nd SR
3-d SR
dF, Hz
lg(W), W/m2
0.7
0.6
0.5
0.4
0.3
0.2
0.1
0
-6.5
-6
-5.5
-5
-4.5
-4
-3.5
-3

Fig10.jpg.

10-09-2017 X8.2 Hy

Mode 3

Hz

21
20.8
20.6
20.4
20.2

Mode 2

Hz

14.8
14.6
14.4
14.2
14
13.8

Mode 1

Hz

8
7.8
7.6
7.4

GOES x-Ray Flux

W/m^2

1e-4
1e-6
1e-8

0.01-0.2 nm
0.01-0.3 nm
0.05-0.5 nm
0.1-0.8 nm

15
16
17
18
19

UT

Fig03.jpg.

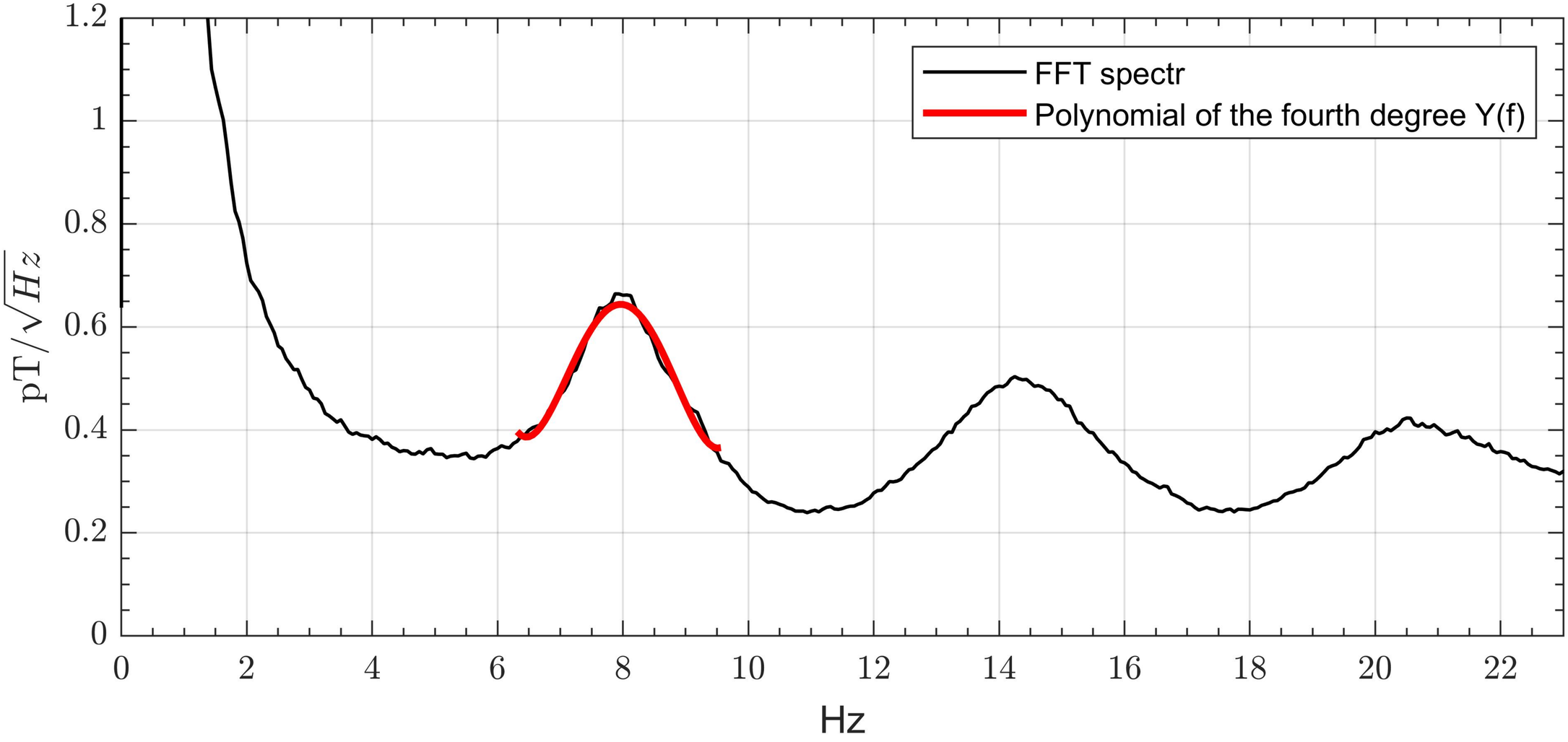
FFT spectr
Polynomial of the fourth degree Y(f)
pT/√Hz
Hz
0
0.2
0.4
0.6
0.8
1
1.2
0
2
4
6
8
10
12
14
16
18
20
22

Fig02.jpg.

10-Sep-2017 Hy

$\mathrm{dB(pT/\sqrt{Hz})}$

Hz

UT, hour

Fig04.jpg.

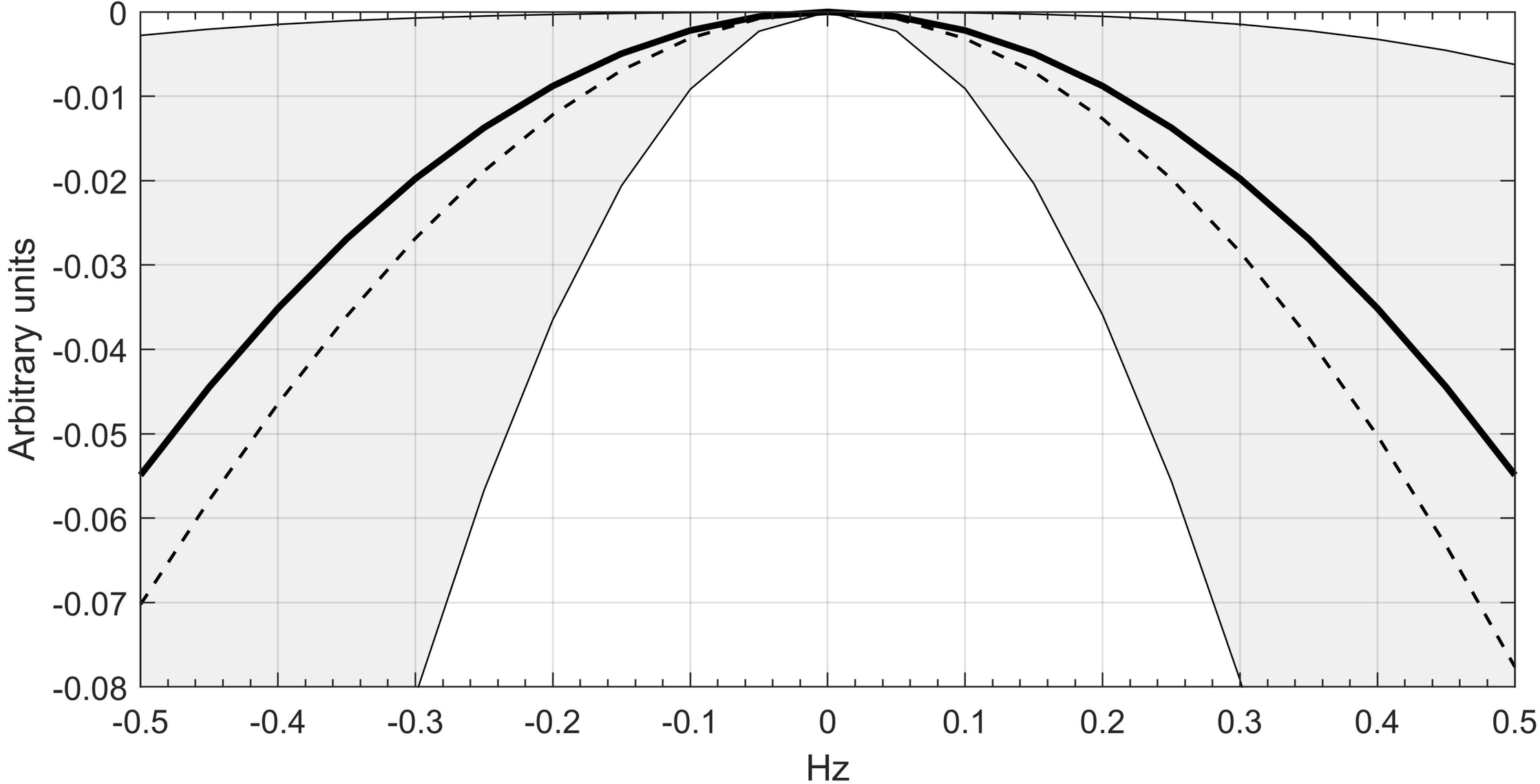
0
-0.01
-0.02
-0.03
-0.04
-0.05
-0.06
-0.07
-0.08
Arbitrary units
-0.5
-0.4
-0.3
-0.2
-0.1
0
0.1
0.2
0.3
0.4
0.5
Hz

Fig06.jpg.

Amplitude

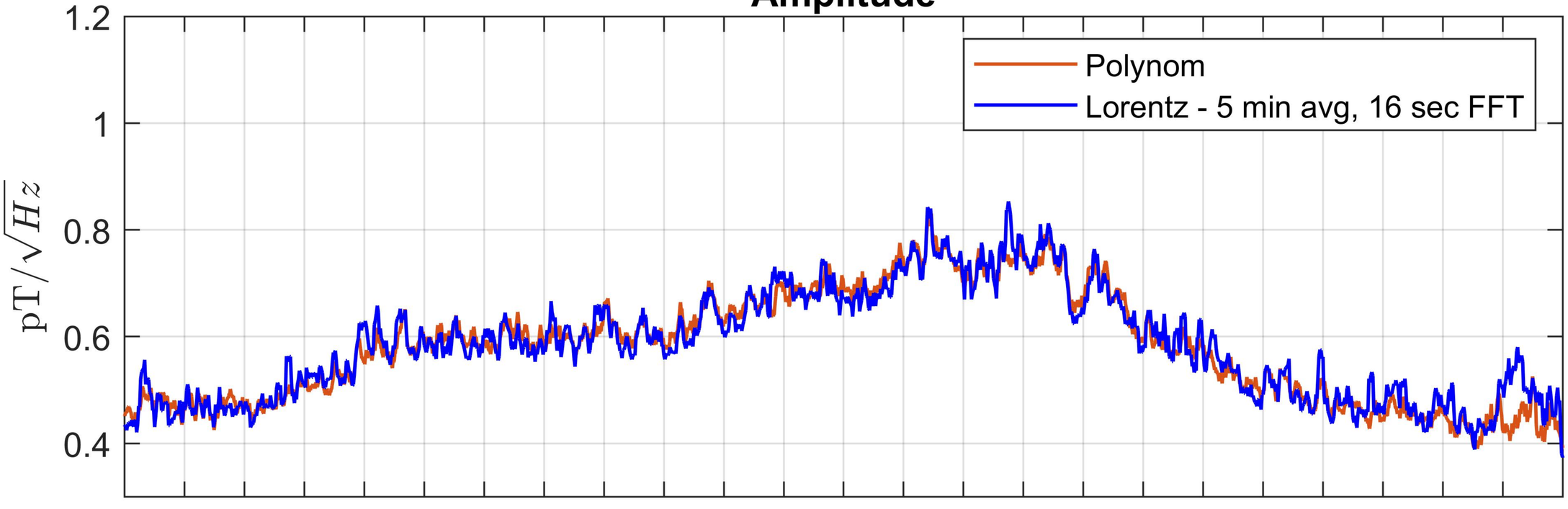

Frequency

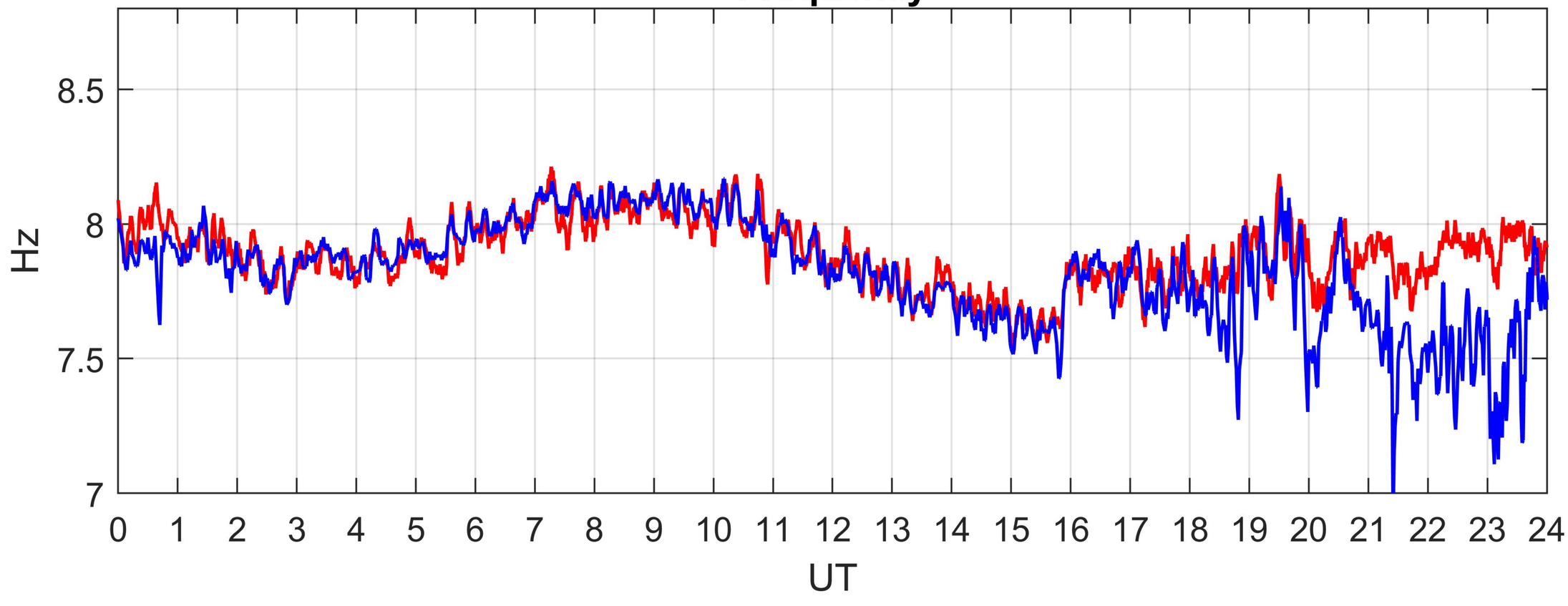

Fig01.jpg.

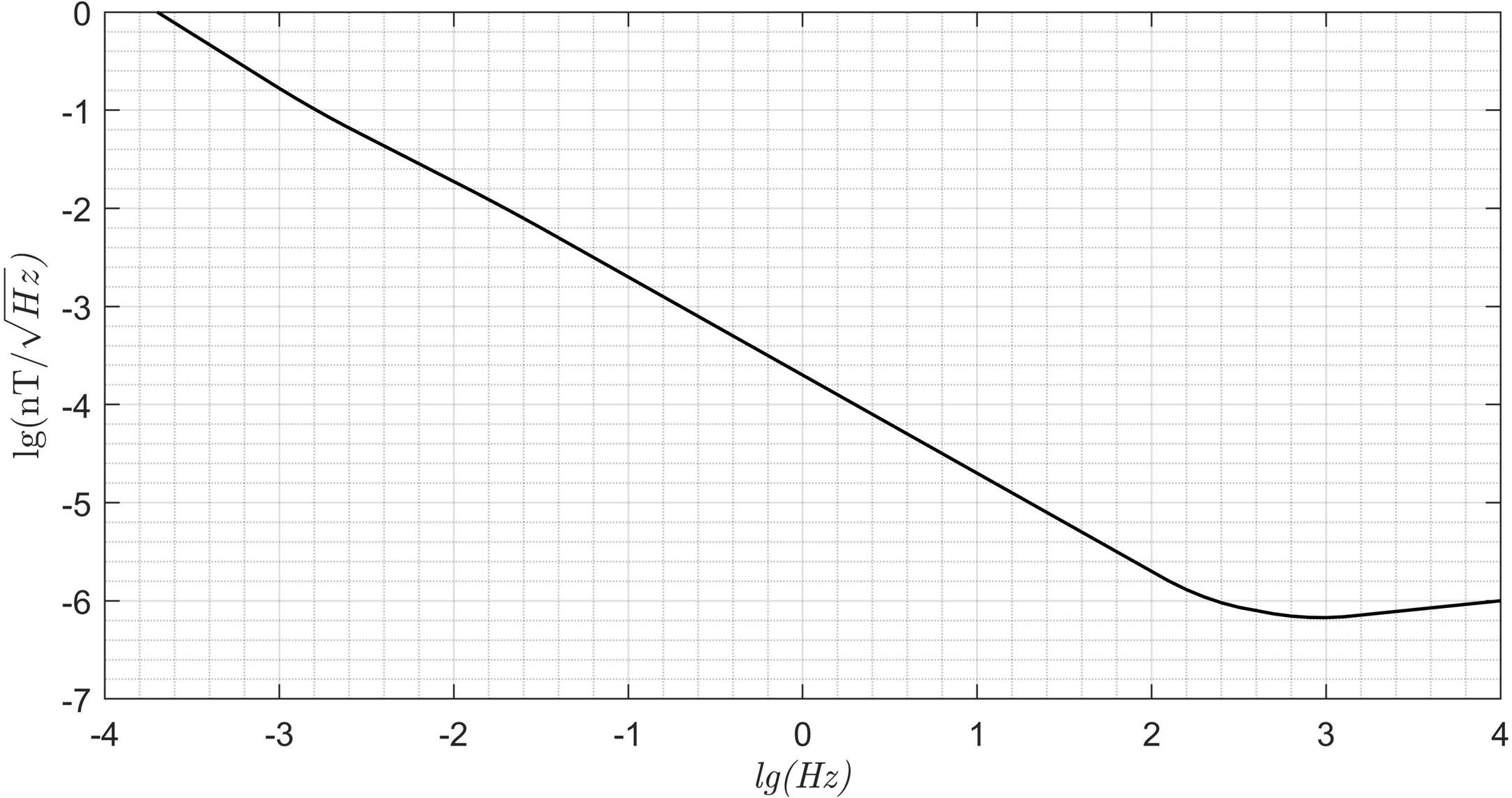
0
-1
-2
-3
-4
-5
-6
-7
$\lg(\mathrm{nT}/\sqrt{Hz})$
-4
-3
-2
-1
0
1
2
3
4
$lg(Hz)$

Fig08.jpg.

10.09.2017 X8.3 Frequency mode 1

Hz

8.2
8
7.8
7.6
7.4

Hx
Hy

Freqequency mode 2

Hz

15
14.5
14
13.5

X-ray

W/m^2

0.001
1e-5
1e-07

0.05-0.4 nm
0.1-0.8 nm

12 13 14 15 16 17 18 19 20 21 22 23 24

UT

Investigation Of The Reaction Of Schumann Resonances To Short Transient Geophysical Events Under The Influence Of Atmospheric Electromagnetic Noise

Yu.V. Poklad[1], I.A. Ryakhovsky[1,2], B.G. Gavrilov[1], V.M. Ermak[1], E.N. Kozakova[1], N.S. Achkasov[1]

[1]Sadovsky Institute of Geospheres Dynamics, Russian Academy of Sciences, Moscow, Russia
[2]Moscow Institute of Physics and Technology, Moscow, Russia

Key Points:

- A new method for calculating the parameters of Schumann Resonance (SR) significantly reduces the impact of electromagnetic interference
- The developed technique increased the temporal resolution of the SR frequency and amplitude data
- The new technique made it possible to establish the dependence of the SR frequency on the X-ray flux with a wavelength of less than 0.2 nm

Corresponding author: Ilia Ryakhovsky, ryakhovskiy88@yandex.ru

Abstract

The Schumann resonance (SR), the source of which is the global thunderstorm activity is constantly observed in the Earth-ionosphere waveguide. Changes in the parameters of SR signals caused by geophysical disturbances make it possible to study the state and dynamics of the lower ionosphere. When calculating the SR parameters, there are problems associated with the impact of electromagnetic interference of natural and anthropogenic origin. The main natural sources of interference are signals associated with the radiation of nearby lightning discharges, as well as the influence of the Alfvén ionospheric resonator. The paper presents a new method for calculating the SR parameters,which significantly reduces the impact of these interferences. The developed technique significantly increased the temporal resolution of the obtained data on the frequency and amplitude of the SR. Due to this, it became possible to study the influence of fast heliogeophysical disturbances (such as solar X-ray flares) on the lower ionosphere and, as a consequence, on the parameters of the SR. An analysis of the experimental data made it possible to establish a linear dependence of the SR frequency on the logarithm of the X-ray flux in the range up to 0.2 nm during a class X solar flare.

1 Introduction

Schumann resonances (SR) are electromagnetic radiation (EMR) that constantly exists in the Earth's atmosphere, the spectrum of which is characterized by the presence of pronounced and fairly stable frequency maxima. In 1952, Schumann (Schumann, 1952) theoretically predicted the existence of resonant modes at frequencies close to 8, 14, 20 ... Hz resulting from interference of low-frequency EMR in the Earth-ionosphere waveguide. Due to their global nature, SR can be reliably recorded in any region on the Earth's surface (Sentman & Fraser, 1991) and are an indicator of global thunderstorm activity on the planet (Clayton & Polk, 1976; Heckman et al., 1998), since the exact values of the frequency of peaks of the SR spectrum are associated with the spatiotemporal distribution and intensity of thunderstorms (Ogawa et al., 1969; Nickolaenko et al., 1998; Prácser et al., 2019; Pizzuti et al., 2022).

SR signals excited by lightning discharges propagate in the Earth-ionosphere waveguide and carry information about both the sources and the propagation parameters of electromagnetic radiation in the Hz range determined by the properties of the upper wall of the waveguide, the D region of the ionosphere. This means that strong heliogeophysical disturbances, such as solar flares, magnetic storms, precipitation of high-energy particles (Schlegel & Füllekrug, 1999), leading to a change in the state of the lower ionosphere, can affect the SR parameters.

The possibility of a correct description of changes in the properties of the waveguide allows, in principle, to solve the inverse problem: determining the effective height of the lower ionosphere, coordinates and intensity of global thunderstorm centers (Sentman & Fraser, 1991; Sentman, 1996).

The main problems arising in the analysis of variations in the amplitude-frequency spectrum of the SR are associated with the noise level of the EMR in the frequency range of the SR. The main sources of electromagnetic noise in this range are noise associated with industrial network radiation at a frequency of 50 Hz and pulse signals associated with atmospheric radiation caused by near lightning discharges. Also, in the frequency range up to 15-20 Hz, effects associated with the ionospheric Alfven resonator can be observed (Demekhov, 2012).

The creation of a technique that makes it possible to reliably clear the SR signals from interference caused by radiation from other sources and to investigate variations in the parameters of the SR signals during geophysical disturbances is the task of this work.

2 Instrumentation and Observation

The "Mikhnevo" Geophysical Observatory (GO) of the Sadovsky Institute of Geospheres Dynamics of the Russian Academy of Sciences (IDG RAS) is located about 100 km south of Moscow (54.96 N, 37.76 E). The observatory is located at a considerable distance from large settlements and industrial facilities. Since 2011, it has been continuously registering electromagnetic signals in the ELF/VLF frequency range (Ryakhovskii et al., 2021). Induction magnetometers Metronix MFS-06 oriented in the direction of magnetic North-South and West-East are used as sensors. For the Mikhnevo Observatory, the local magnetic declination is 9 degrees. Registration is carried out on a 10-channel 24-bit Metronix ADU-07 logger with a digitization frequency of 256 Hz. Time binding is carried out by means of GPS with an accuracy of 30 ns. The equipment is located at a distance of about 500 m from the nearest sources of the power grid. MFS-06 magnetometers have a low intrinsic noise level. The graph of the dependence of the noise level of the MFS-06 magnetometers on the frequency is shown in Figure 1.

The low level of industrial noise in the GO "Mikhnevo", high sensitivity and a wide dynamic range of equipment allow you to receive ultra-weak signals. All the source data for the period from 2011 to the present are stored in the wave forms on the server of the IDG RAS.

An example of the frequency spectrum in the frequency range from 0 to 50 Hz obtained by processing the daily recording of the signal of the Hy magnetic field component (East-West) for September 10, 2017 is shown in Figure 2. The first five or six Schumann resonances are well traced. After 16 hours, characteristic "ascending" maxima associated with the ionospheric Alfven resonator are visible in the range of 1-15 Hz. Starting from 18 UT, they begin to overlap the first mode of the Schumann resonator.

One of the main obstacles in determining the parameters of Schumann resonances are spherics, which are signals from lightning discharges. This is due to the fact that the spherics spectrum is broadband and is also present at Schumann frequencies. Their characteristic duration ranges from units to tens of milliseconds. In Figure 2 (lower panel), close spherics are visible as bright vertical lines.

3 Method of Calculation

Usually, the Lorentz functions are successfully used to restore the parameters of Schumann resonances (Sentman, 1987; Roldugin et al., 2003). To minimize the influence of signals from lightning discharges and other interference, we have developed a new algorithm for calculating the parameters of Schumann resonances, the results of which are shown by the example of processing the recording of the Hy component of the magnetic field for 10.09.2017.

To obtain the amplitude spectrum, the Welch method is used (Welch, 1967). This procedure is described in detail in Rodriguez-Camacho et al. (2018). We are working with a time window of 16 seconds and a time swapping between adjacent windows time equal to 3 seconds. To smooth the effect of abrupt end we use Hann window.

The degree of distortion of the spectrum by spherics signals was estimated by comparing them with the "reference" spectrum. The reference spectrum was obtained by averaging the spectra calculated from short samples over a four-hour time period. The results of calculating the "reference" spectrum of the first three Schumann resonances for the time period from 08:40 to 12:40 UT are shown in Figure 3. This figure shows that the 1st Schumann resonance occupies the frequency band from 6.3 to 9.6 Hz. Table 1 shows the frequency ranges occupied by the first four modes of Schumann resonances.

Table 1. Valid Ranges for the Fitting Parameters Under Regular Behavior

SR Number	SR bands, Hz	Valid SR frequency, Hz
1	6.3-9.6	6.8-9.1
2	12.2-16.3	12.9-15.6
3	18.0-22.8	18.9-21.9
4	23.5-29.5	24.6-28.4

In these frequency bands the approximation of experimental data was carried out by a polynomial of the fourth degree:

$$Y(f) = af^4 + bf^3 + cf^2 + df + e \tag{1}$$

The results of approximation of the first SR are shown in Figure 3 of the red curve. Based on (1), the frequency value f_0 of the first SR is determined from the following conditions:

$$\begin{cases} Y'(f_0) = 0 \\ Y''(f_0) < 0 \end{cases} \tag{2}$$

For the convenience of further use, the "reference" curve of the spectrum of the 1^{st} SR can be represented by the following expression:

$$Y_0(f) = Y(f + f_0) - Y(f_0) \tag{3}$$

The $Y_0(f)$ function is shown in Figure 4 as a solid black curve.

Further, similar calculations (equations 1-3) were carried out for the spectra obtained from short 16 second samples. The approximation was considered correct and was used further if the approximating polynomial $I_0(f)$ had only one maximum. Examples of such an approximation are presented in Figure 4 by the black dotted curve. Also we take into account only such polinomian, for which f_0 lies in the valid SR frequency band shown in Table 1.

As a measure of the difference between the approximation of the 16-second spectrum and the reference one, the relative difference in the values of the integrals in the range of -0.5 to 0.5 Hz from the maximum was chosen:

$$Err = \frac{\int_{-0.5}^{0.5} I_0(f)\mathrm{d}f - \int_{-0.5}^{0.5} Y_0(f)\mathrm{d}f}{\int_{-0.5}^{0.5} Y_0(f)\mathrm{d}f} \tag{4}$$

To minimize the influence of samples distorted by spherics signals and other noises, a weighting factor was assigned to each sample. The dependence of the weighting coefficient on the Err parameter is shown in Figure 5. The area in which the weight function is greater than zero is shown in Figure 4 in gray. Next, all the parameters of the Schumann resonances were averaged taking into account the obtained weighting coefficients W.

For example, to obtain the time dependence of the SR frequency with a 5-minute time resolution, we must average 100 values, because they are taken in increments of 3 seconds. Averaging was carried out according to equation:

$$F_0 = \frac{\sum f_{0i} \cdot W_i}{\sum W_i} \tag{5}$$

where f_{0i} are the frequencies of the first Schumann resonance calculated from 16 second spectra, and W_i are the weight coefficients of these spectra. SR amplitudes are calculated in a similar way.

Figure 6 of the red curve shows the time course of the amplitude (upper panel) and frequency (lower panel) of the 1st Schumann resonance on 10.06.2017, obtained from samples satisfying equation 4, averaged over 300 seconds. The blue color shows the values of these parameters obtained with the same 300-second averaging of spectral data calculated using the FFT with a sample of 16 seconds and approximated by the Lorentz function according to the method described in Rodríguez-Camacho et al. (2018). At the same time, an increase in noise is observed on the SR frequency graph after 18 hours on the blue curve, which is due to the fact that the recording of the frequency variation of the first and partially second SR is distorted by the influence of signals at the frequency of the ionospheric Alfven resonator. The use of our technique allowed us to correctly restore the amplitude - frequency characteristics of the first SR during this period of time.

The developed spherics filtering technique can also be applied to the recovery of SR parameters using Lorentz functions. To do this, we averaged 16-second spectra cleared of spherics at a 5-minute interval, taking into account the weighting coefficients, and then the resulting spectrum was fitted with Lorentz functions. The result of such processing is shown in Figure 7.

It can be seen that the application of our technique for excluding spectral data containing spherics and other noises makes it possible to significantly neutralize the influence of the ionospheric Alfven resonator on the calculation of SR parameters.

4 Results and discussion

The developed technique significantly increased the time resolution of the frequency and amplitude data of the SR. Thanks to this, it became possible to study the influence of short-term heliogeophysical disturbances (such as Solar flares) on the lower ionosphere and, as a consequence, on the parameters of the SR. Figures 8 and 9 show the reaction of the first two SR frequencies to X-ray flashes of X and M class. The upper and middle panels show the time course of the frequency of the first two SR modes, and the lower one shows the flux of hard X-ray radiation in the ranges of 0.05–0.4 and 0.1–0.8 nm according to the GOES satellite. Thanks to the purification of the original signal from interference in the form of spherics, it was possible to trace the reaction of the Schumann resonator not only to X-class flashes, but also to weaker M-class flashes (Poklad et al., 2018).

The dependences of the frequency variations of the Schumann resonances on the radiation flux in different spectral ranges for the X8.2 class flash that occurred on 10.09.2017 were also obtained.

According to the ratio of X-ray radiation fluxes recorded on the GOES-15 satellite in the spectral ranges 0.05-0.4 nm and 0.1-0.8 nm, the brightness temperatures of the source were calculated under the assumption of solar radiation as an absolutely black body. Using this temperature according to the Planck formula, we calculated the radiation flux in the ranges 0.01-0.2 nm and 0.01-0.3 nm (bottom panel of Figure 10). To calculate the deviation of the frequency of the Schumann resonance from the data correct at 2 hours before the start of the solar flare and 2 hours after its end (i.e. during the times 13:41-15:41 and 17:55-19:55 UT), a trend was built using a 2nd degree polynomial. Figure 10 shows the time course of the Schumann resonance frequency as a solid curve, and its trend as a dotted line.

Figure 11 shows the dependences of the variations in the frequency of the SR on the logarithm of the radiation flux in different spectral ranges. The thick curve shows

the dependencies for the leading edge of the flash. The point at which the radiation flux was 0.01 of the maximum value in the same spectral range was taken as the beginning of the front. The duration of the leading edge of the flash was from 10.6 minutes in the range of 0.01-0.2 nm to 18 minutes in the range of 0.1-0.8 nm, which exceeds the time window for calculating the parameters of the SR, which was 5 minutes. The thin curve shows the dependencies for the rear edge of the flash. For the range 0.01-0.2 nm, the point at which the radiation flux dropped to 0.01 from the maximum (17:10 UT) was taken as the end of the front. For the remaining ranges, the end of the flash was considered to be the time at 18:00 UT.

Figure 11 shows that at the leading edge of the flash, the variations in the frequency of the SR linearly depend on the radiation flux. For ranges 0.01-0.2 nm regression coefficients at the rear edge of the flash are close to those obtained at the front. From this it can be concluded that the X-ray flux in the range up to 0.2 nm is the determining factor for calculating the effect of solar flares on the parameters of the SR. The approach proposed in this paper to the study of the reaction of SR signals to geophysical disturbances, including an effective method of filtering interference associated with thunderstorm atmospherics and other noise sources, allowed us to study the reaction of the Schumann resonator to a wide range of ionospheric disturbances. In the article, these possibilities are demonstrated by the example of solar X-ray flares. Further development and application of this technique will make it possible to study the reaction of the Schumann resonator to other fast-flowing heliogeophysical disturbances.

Acknowledgments

This work was supported by the Ministry of Science and Higher Education of the Russian Federation, project no. 1021052706243-1-1.5.9;1.5.1.

References

Clayton, M. D., & Polk, C. (1976). Diurnal variation and absolute intensity of world-wide lightning activity, september 1970 to may 1971..

Demekhov, A. G. (2012, JUN). Coupling at the Atmosphere-Ionosphere-Magnetosphere Interface and Resonant Phenomena in the ULF Range [Review]. *SPACE SCIENCE REVIEWS*, *168*(1-4), 595-609. doi: {10.1007/s11214-011-9832-6}

Heckman, S. J., Williams, E., & Boldi, B. (1998). Total global lightning inferred from schumann resonance measurements. *Journal of Geophysical Research: Atmospheres*, *103*(D24), 31775-31779. Retrieved from `https://agupubs.onlinelibrary.wiley.com/doi/abs/10.1029/98JD02648` doi: https://doi.org/10.1029/98JD02648

Nickolaenko, A. P., Sátori, G., Zieger, B., Rabinowicz, L. M., & Kudintseva, I. G. (1998). Parameters of global thunderstorm activity deduced from the long-term schumann resonance records. *Journal of Atmospheric and Solar-Terrestrial Physics*, *60*, 387-399.

Ogawa, T., Tanka, Y., & Yasuhara, M. (1969). Schumann resonances and worldwide thunderstorm activity. *Journal of geomagnetism and geoelectricity*, *21*(1), 447-452. doi: 10.5636/jgg.21.447

Pizzuti, A., Bennett, A., & Füllekrug, M. (2022). Long-term observations of schumann resonances at portishead (uk). *Atmosphere*, *13*(1), 38.

Poklad, Y. V., Ermak, V. M., & Ryakhovskiy, I. A. (2018). Influence of local time and power of solar x-ray flashes of M and X classes on the variation of frequency of first mode of Schumann resonance. In G. G. Matvienko & O. A. Romanovskii (Eds.), *24th international symposium on atmospheric and ocean optics: Atmospheric physics* (Vol. 10833, pp. 2091 – 2094). SPIE. Retrieved from `https://doi.org/10.1117/12.2504511` doi: 10.1117/12.2504511

Prácser, E., Bozoki, T., Sátori, G., Williams, E., Guha, A., & Yu, H. (2019, 03). Reconstruction of global lightning activity based on schumann resonance measurements: Model description and synthetic tests. *Radio Science*, *54*. doi: 10.1029/2018RS006772

Rodríguez-Camacho, J., Fornieles, J., Carrión, M. C., Portí, J. A., Toledo-Redondo, S., & Salinas, A. (2018, December). On the Need of a Unified Methodology for Processing Schumann Resonance Measurements. *Journal of Geophysical Research (Atmospheres)*, *123*(23), 13,277-13,290. doi: 10.1029/2018JD029462

Rodriguez-Camacho, J., Fornieles, J., Carrion, M., Portí, J., toledo redondo, S., & Salinas Extremera, A. (2018, 11). On the need of a unified methodology for processing schumann resonance measurements. *Journal of Geophysical Research: Atmospheres*, *123*. doi: 10.1029/2018JD029462

Roldugin, V. C., Maltsev, Y. P., Vasiljev, A. N., Shvets, A. V., & Nikolaenko, A. P. (2003). Changes of schumann resonance parameters during the solar proton event of 14 july 2000. *Journal of Geophysical Research: Space Physics*, *108*(A3). Retrieved from `https://agupubs.onlinelibrary.wiley.com/doi/abs/10.1029/2002JA009495` doi: https://doi.org/10.1029/2002JA009495

Ryakhovskii, I. A., Gavrilov, B. G., Poklad, Y. V., Bekker, S., & Ermak, V. (2021). The state and dynamics of the ionosphere from synchronous records of ulf/vlf and hf/vhf radio signals at geophysical observatory "mikhnevo". *Izvestiya, Physics of the Solid Earth*, *57*, 718-730.

Schlegel, K., & Füllekrug, M. (1999). Schumann resonance parameter changes during high-energy particle precipitation. *Journal of Geophysical Research*, *104*, 10111-10118.

Schumann, W. O. (1952, February). Über die strahlungslosen Eigenschwingungen einer leitenden Kugel, die von einer Luftschicht und einer Ionosphärenhülle umgeben ist. *Zeitschrift Naturforschung Teil A*, *7*(2), 149-154. doi: 10.1515/zna-1952-0202

Sentman, D. D. (1987). Magnetic elliptical polarization of schumann resonances. *Radio Science*, *22*(04), 595-606. doi: 10.1029/RS022i004p00595

Sentman, D. D. (1996). Schumann resonance spectra in a two-scale-height earth-ionosphere cavity. *Journal of Geophysical Research: Atmospheres*, *101*(D5), 9479-9487. Retrieved from `https://agupubs.onlinelibrary.wiley.com/doi/abs/10.1029/95JD03301` doi: https://doi.org/10.1029/95JD03301

Sentman, D. D., & Fraser, B. J. (1991). Simultaneous observations of schumann resonances in california and australia : evidence for intensity modulation by the local height of the d region. *Journal of Geophysical Research*, *96*, 15973-15984.

Welch, P. (1967). The use of fast fourier transform for the estimation of power spectra: A method based on time averaging over short, modified periodograms. *IEEE Transactions on Audio and Electroacoustics*, *15*(2), 70-73. doi: 10.1109/TAU.1967.1161901

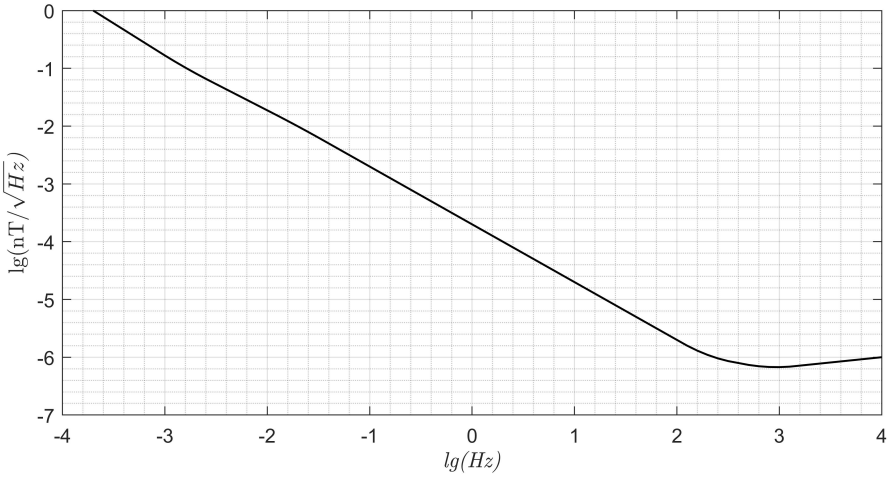

Figure 1. The Equivalent Magnetic Field Noise of MFS-06 magnetometers

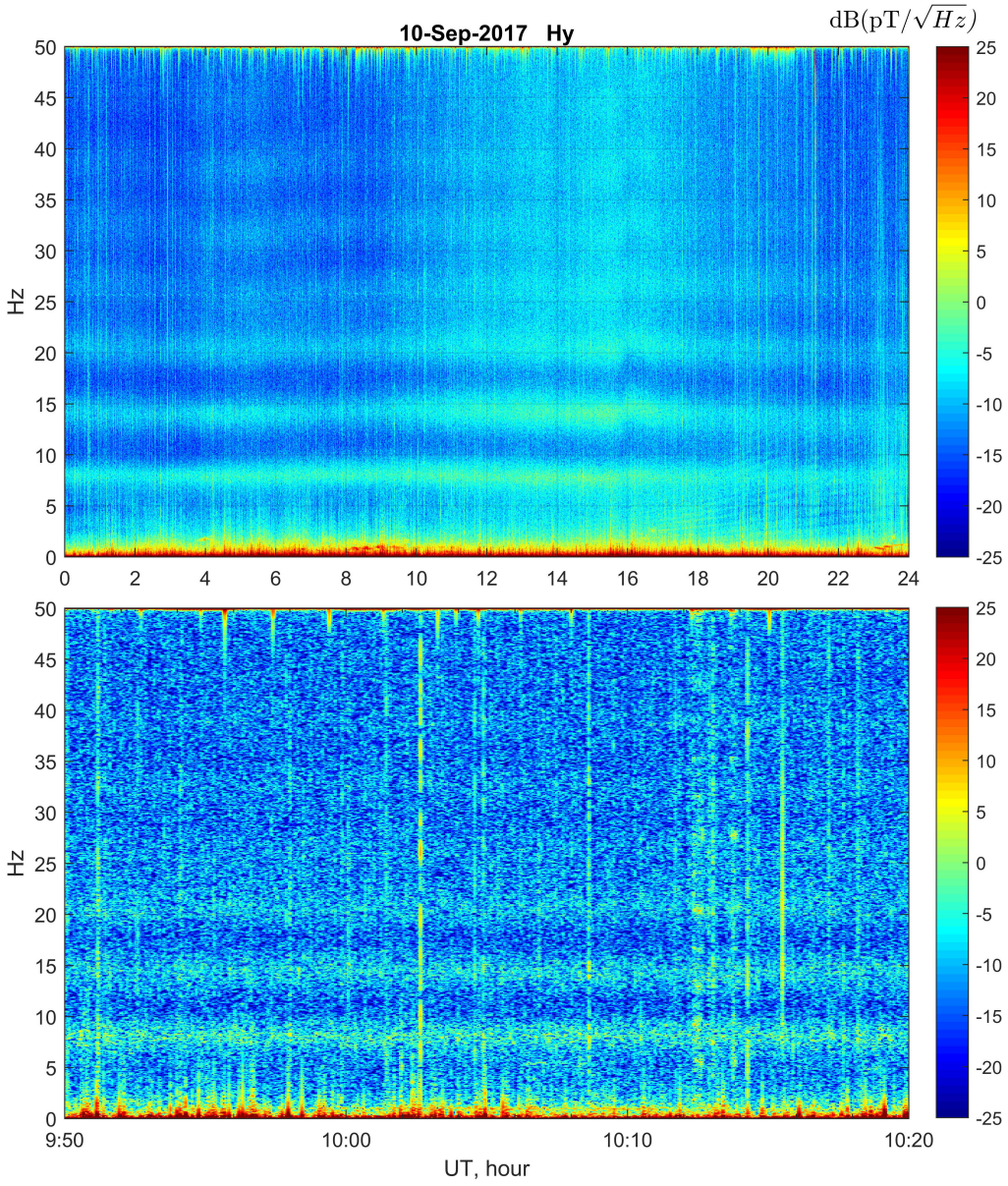

Figure 2. Daily recording of the EMR variation in the frequency range from 0 to 50 Hz, registered in the GO "Mikhnevo" on 10.09.2017 (upper panel), a fragment of the recording from 09:50 to 10:30 UT (lower panel)

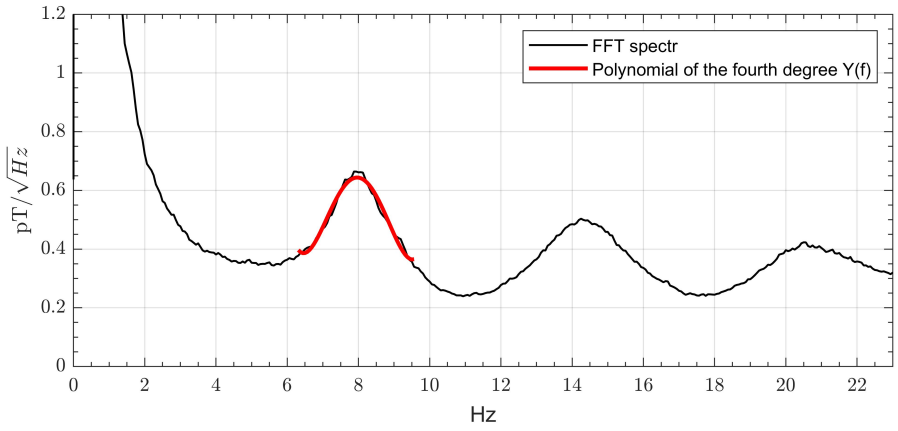

Figure 3. The black curve is the "reference" spectrum of the first three SR, calculated over a 4-hour period (from 08:40 to 12:40 UT) for 10.09.2017, the red curve is an approximation of the first SR by a polynomial of the fourth degree in the frequency band from 6.3 to 9.6 Hz

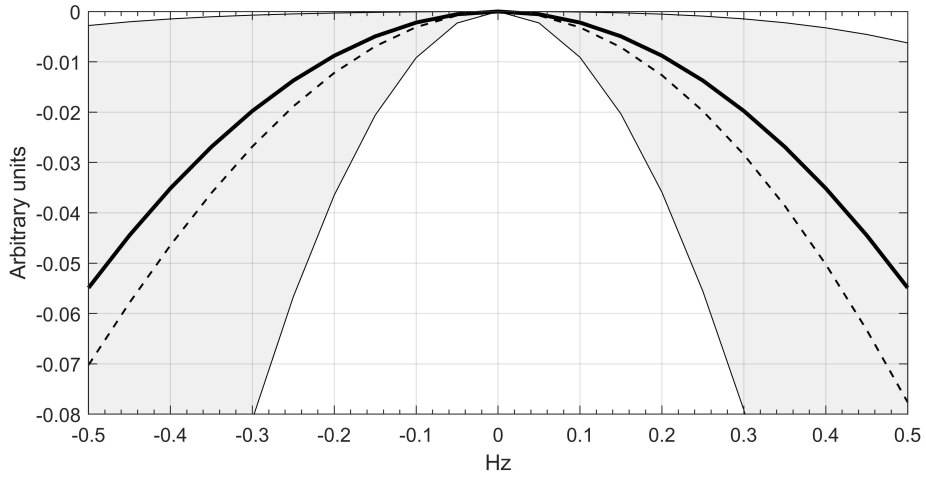

Figure 4. The black curve is the result of approximation of the "reference" spectrum by a fourth-degree polynomial $Y_0(f)$, the black dotted curve is the result of approximation of the spectrum calculated from a 16-second sample by a fourth-degree polynomial $I_0(f)$, the area satisfying criterion (4) is marked in gray

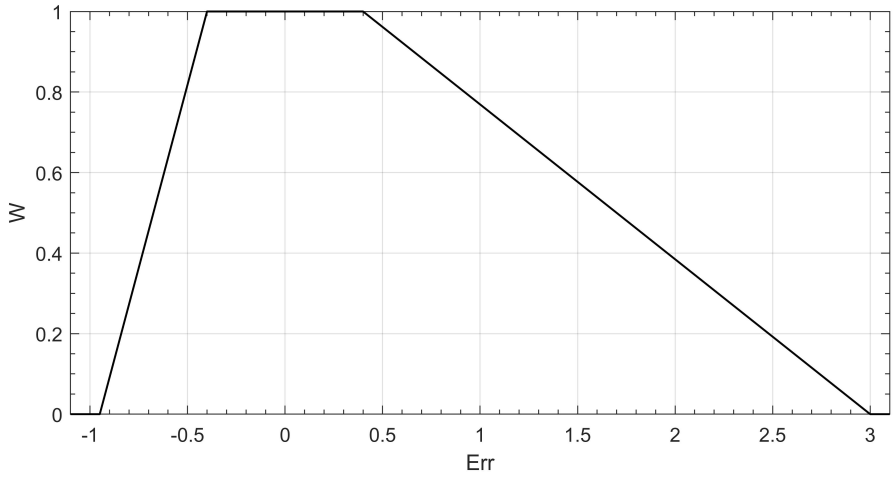

Figure 5. The dependence of the weight coefficient on the value Err parameter

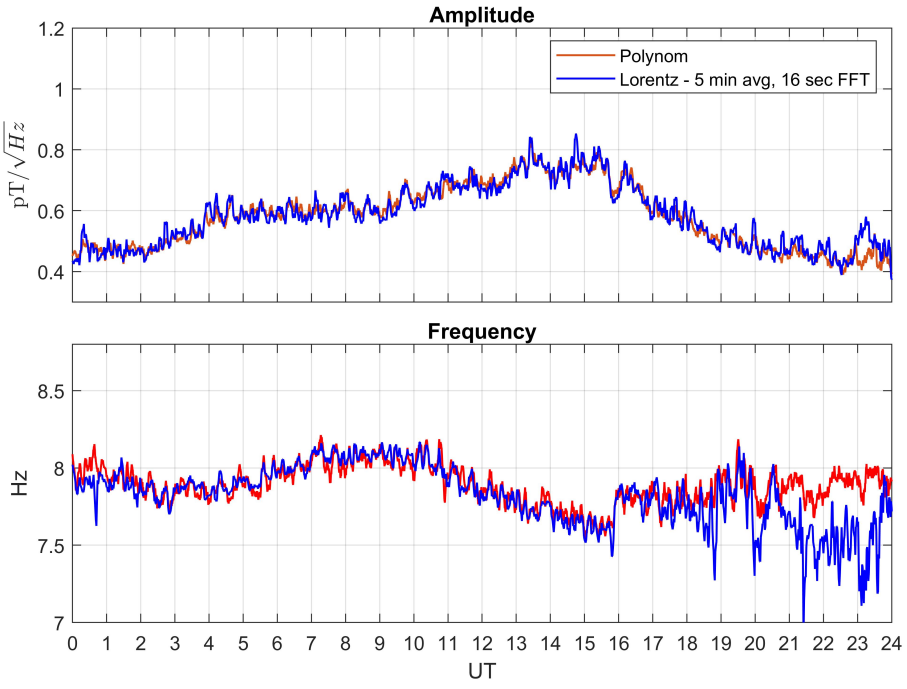

Figure 6. The time course of the amplitude of the 1st SR (upper panel) and frequency (lower panel) for 10.06.2017, calculated using the Lorentz functions (blue curves) and using our methodology (red curves)

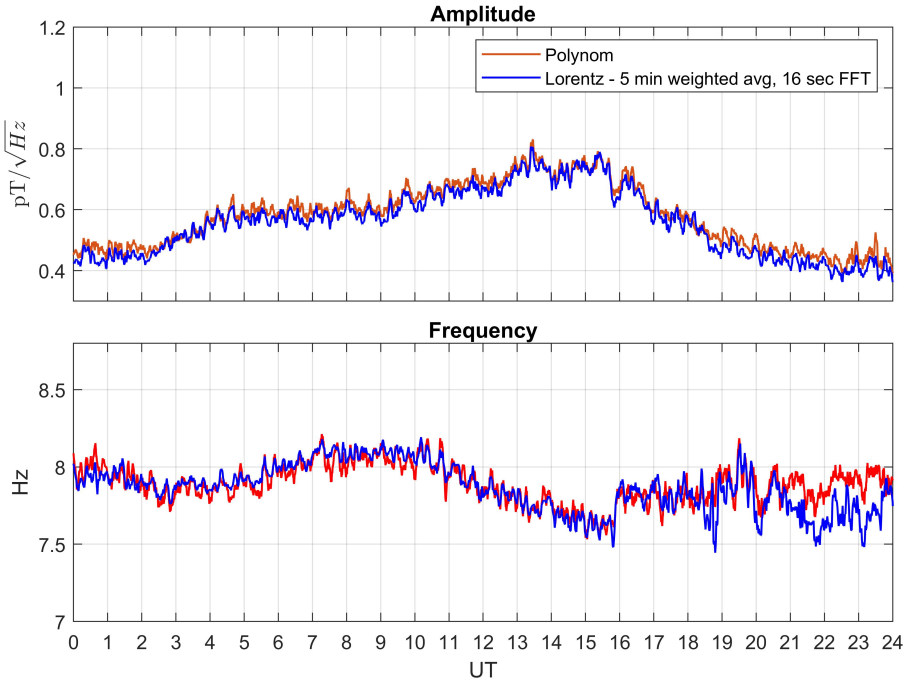

Figure 7. The time course of the amplitude of the 1st SR for 10.06.2017 (upper panel), calculated using Lorentz functions from spectra cleared from spherics (blue curve) and using our methodology (red curve). The time course of the frequency (lower panel, calculated using Lorentz functions from spectra cleared from spherics (blue curve) and using our methodology (red curve)

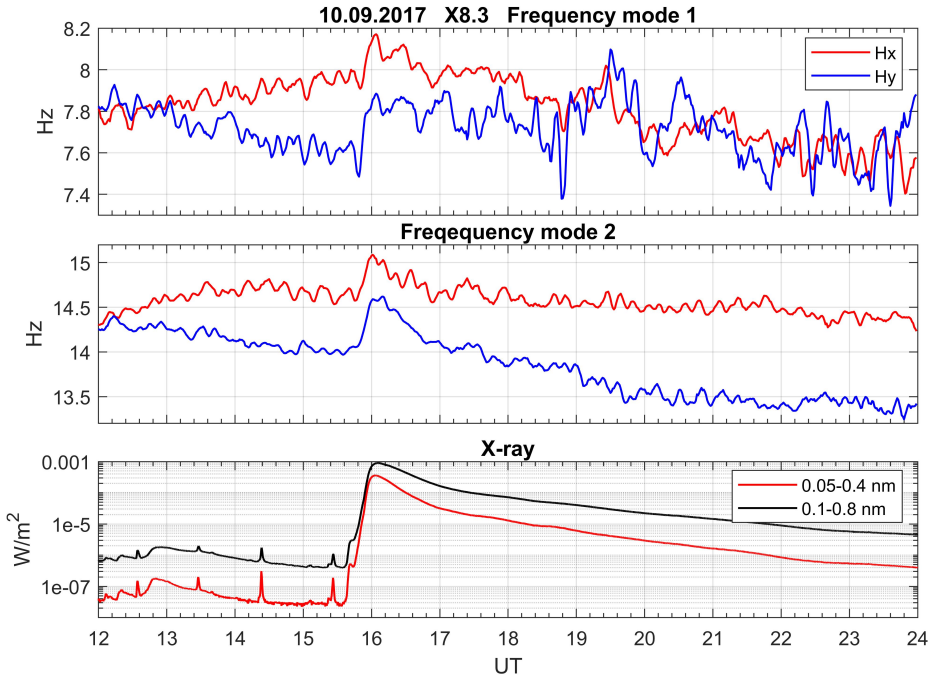

Figure 8. Frequency response of the first (upper panel) and second (middle panel) SR to a solar flare of Class M4.2 (lower panel) 12.03.2015.

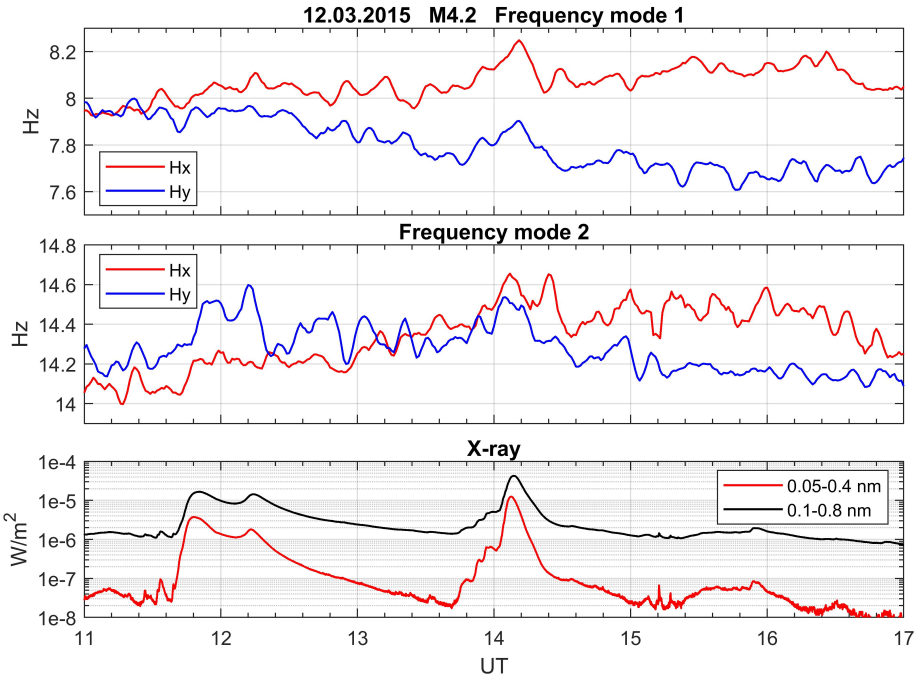

Figure 9. Frequency response of the first (upper panel) and second (middle panel) SR to a solar flare of class X8.3 (lower panel) on 10.09.2017.

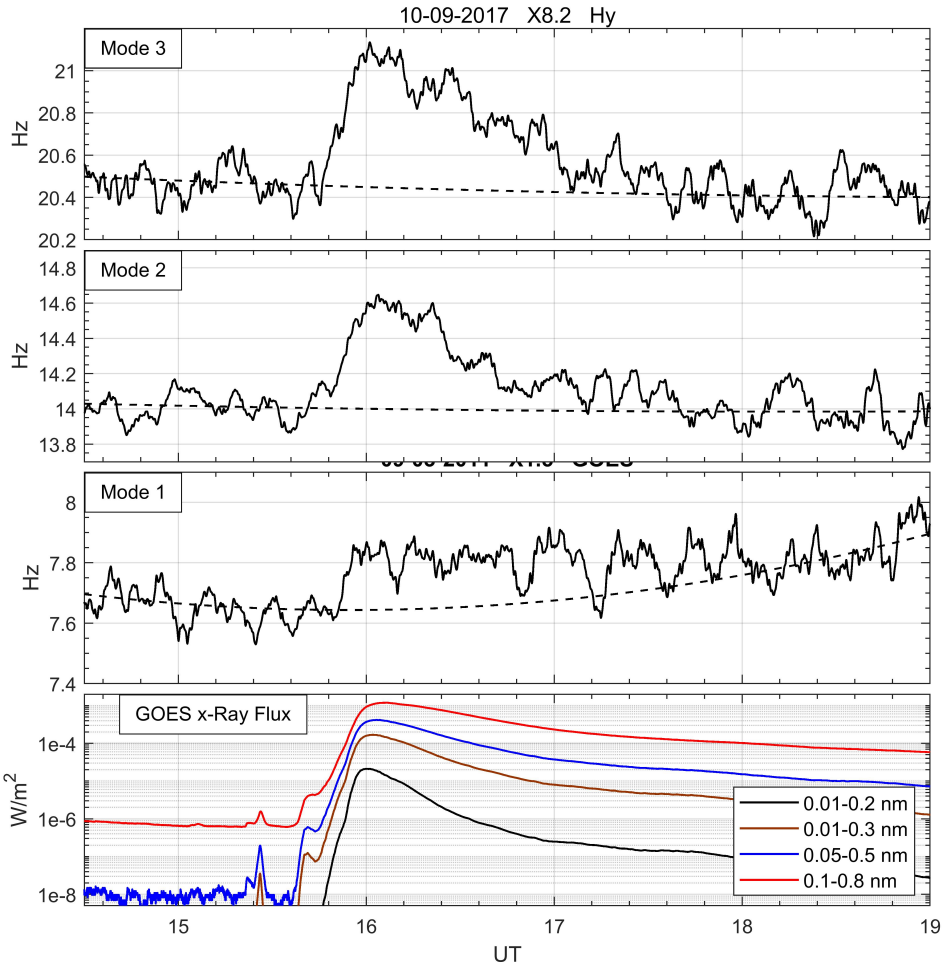

Figure 10. Frequency variation of the first, second and third Schumann resonances during the solar flare X8.2. 10.09.2017.

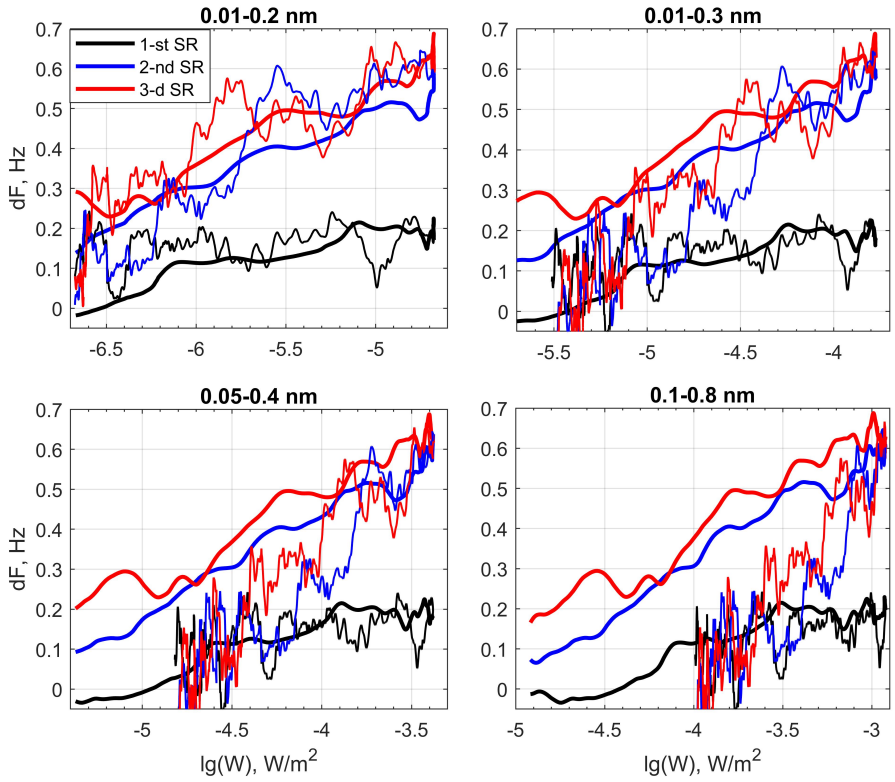

Figure 11. Dependences of frequency variations of the first three Schumann resonances on the logarithm of the radiation flux in different spectral ranges